Journal of Energy and Safety Technology

JEST

RESEARCH ARTICLE Open Access

PERFORMANCE STUDY ON THE HYBRID SYSTEM OF PIEZOELECTRIC-TRIBOELECTRIC NANOGENERATORS

Nor Al Danish Nor Azaman[1], Norzanah Rosmin[1]*, Norhafezaidi Mat Saman[2], Madihah Md Rasid[1], Aripriharta[3], Muhammad Daniel Muhammad Zulkepli[1] & Mohd Hafiz Habi Buddin[1]

[1]Centre of Electrical Energy Systems (CEES), Institute of Future Energy (IFE), Universiti Teknologi Malaysia, 81310 Johor Bahru, Johor, Malaysia.
[2]Institute of High Voltage and High Current, Faculty of Electrical Engineering, Universiti Teknologi Malaysia, 81310 Johor Bahru, Johor, Malaysia.
[3]Department of Electrical Engineering, Universitas Negeri Malang, Malang 65145, Indonesia

*Corresponding author: norzanah@utm.my

Article History

Received:	Received in revised form:	Accepted:	Published:
June 3, 2025	July 22, 2025	July 22, 2025	December 12, 2025

Abstract

The global shift towards renewable and sustainable energy sources has intensified interest in modern energy harvesting technologies, particularly for low-power electronic applications. However, conventional single-mode energy harvesters, such as standalone piezoelectric nanogenerators (PENGs) or triboelectric nanogenerators (TENGs), face limitations in energy conversion efficiency and consistency under varying mechanical conditions. This study addresses these limitations by proposing a hybrid nanogenerator system that integrates both piezoelectric and triboelectric mechanisms to enhance overall performance. The main objective is to evaluate the energy harvesting efficiency and output characteristics of the hybrid nanogenerator system under different operating scenarios. The hybrid design aims to maximize electrical output and improve system reliability by combining the piezoelectric effect, which converts mechanical stress into electrical energy with the triboelectric effect, which harnesses kinetic energy through contact electrification and electrostatic induction. To achieve this, the system is modeled and simulated using COMSOL Multiphysics and MATLAB Simulink. The PENG component is evaluated based on different materials (PVDF and PZT-5H) and applied mechanical forces, while the TENG component is analyzed under various operational modes (single-electrode and contact-separation). A circuit-level prototype simulation is developed using full-wave bridge rectifier (FWBR) configurations to examine AC-to-DC conversion efficiency and potential for energy storage in lithium-ion batteries. The simulation results reveal that PVDF-based PENGs generate higher voltage output than those made from PZT-5H. For TENGs, the contact-separation mode yields significantly better voltage output than the single-electrode mode. The integration of both nanogenerator types, along with effective rectification, demonstrates the system's capability to produce stable DC output suitable for powering portable and wearable electronics. This study contributes to the advancement of self-powered technologies by providing valuable insights into the design and optimization of hybrid nanogenerators for practical, scalable energy harvesting solutions.

Keywords: Piezoelectric Nanogenerators; Triboelectric Nanogenerators; Hybrid Nanogenerators; Energy Storage.

1.0 INTRODUCTION

As global energy consumption increases, there is a crucial need for sustainable and environmentally friendly alternative energy sources. Conventional energy generation methods frequently depend on fossil fuels, which result in climate change and environmental degradation. As the fossil fuels such as natural gas and coals are burned, they release huge amounts of carbon dioxide and also greenhouse gases into the atmosphere, which lead to global warming. In this context, nanogenerators which apply mechanisms of piezoelectric and triboelectric, which harness ambient mechanical energy, provide a promising solution. The ability of piezoelectric nanogenerators (PENGs) and triboelectric nanogenerators

(TENGs) to transform mechanical energy into electrical energy has drawn interest among the various types of nanogenerators [1]. By transforming mechanical energy from everyday activities like vibrations and walking into electrical energy, these technologies can help to create a more sustainable energy environment [2][3].

According to the theory or the mechanism of piezoelectricity, which states that some materials generate an electric charge when mechanical stress or force is applied [4]. Numerous applications, such as energy harvesters, sensors and also actuators utilized extensive use of this phenomenon. Materials with high piezoelectric coefficients, endurance and adaptability to various conditions, such as lead zirconate titanate (PZT-5H) and polyvinylidene fluoride (PVDF) are commonly used. Triboelectric nanogenerators, which operate based on the triboelectric effect, became a popular and effective energy harvesting technique. When two materials with dissimilar electrons affinities come into contact and then separate, resulting in a transferring charge causing generation of electric potential known as voltage, this phenomenon is known as triboelectric effect [5]. TENGs can effectively capture mechanical energy from vibration, motion and environmental sources due to the triboelectric effect and also electrostatic induction mechanism. TENG can function in various working modes such as single-electrode mode, contact separation mode, sliding mode and free-standing mode [6]. Compact designs can benefit from single-electrode mode since it simplifies the structure of the devices and integration procedure. Next, because of the higher charge density produced during contact and separation cycles, the contact separation mode promotes improved and enhanced output performance. These two working modes are chosen in this paper for further studies.

After important development, a number of issues still need to be addressed, which impedes the wider implementation of these technologies in real-world applications. The performance of PENGs is affected by several factors such as the geometry of the device, the amount and frequency of applied mechanical stress and also the important one is the choice of piezoelectric material. Recent studies have demonstrated that PENGs can effectively harvest energy from low-frequency mechanical inputs, making them suitable for various settings, including wearable electronics [7]. Because of inherent material constraints and inadequate structural designs, PENGs commonly have output voltages and currents that are too low for real-world applications. Despite their widespread use, materials like PZT-5H and PVDF have been found in studies to have performance limitations under specific mechanical stresses, which lowers their energy conversion efficiency [8]. Innovative methods of structural optimization and material engineering are needed to overcome these problems.

Through contact electrification and electrostatic induction, TENGs capture mechanical energy, which providing an efficient way of transforming mechanical energy from the environment into electrical power. Unfortunately, the output voltage produced by TENGs is heavily reliant on the operating or working mode used, which can be a big impact on their overall performance. Every mode has their specifically benefits and limitations that influence the output voltage generated. For example, because of the efficient charge separation that is achieved during the contact separation mode, the vertical contact-separation mode usually produces larger voltages [9]. The single-electrode mode frequently produces lower output voltages than the contact separation mode because of it use ground as a reference electrode [10].

The integration of combining multiple energy harvesting mechanisms such as piezoelectric and triboelectric nanogenerators into a single hybrid system addresses a solution to overcome these challenges. This combination may improve the total energy conversion efficiency by utilizing the complementary characteristics and the strength of each technology [11]. In addition, piezoelectric nanogenerators (PENGs) are efficient under particular mechanical stresses, while triboelectric nanogenerators (TENGs) can function well in a variety of situations such as varying forces and pressures [12]. Thus, combining these two technologies in a single hybrid system can result in a more efficient system that can generate power in response to a wider variety of stimuli. However, aligning their operational principles highlights major challenges. For example, triboelectric systems rely on charge transfer through electrostatic induction and contact electrification, while piezoelectric systems rely on stress-induced charge creation. Designing circuits that maximize energy production while maintaining system stability and ensuring material compatibility are critical study areas [8][13]. Although hybrid nanogenerators systems have advanced, there still remains a gap or lack of understanding regarding the best materials and configurations that will maximize output performance under various operating conditions [12]. Therefore, in this study, the performance of the hybrid nanogenerator is executed to investigate its performance when different materials and different forces are applied to the proposed system.

While numerous studies have investigated piezoelectric nanogenerators (PENGs) and triboelectric nanogenerators (TENGs) individually, as well as in hybrid configurations, many existing works tend to focus on either structural innovations or general performance improvements without systematically evaluating the best-performing material-mode combinations or rectification strategies. Recent hybrid systems often combine PENG and TENG mechanisms to enhance overall output, but they frequently lack optimization of the input parameters and output circuitry [5][6]. This study seeks to bridge that gap by conducting a comprehensive performance evaluation that compares several piezoelectric materials specifically PVDF and PZT-5H as well as different TENG working modes, including single-electrode and contact-separation. The goal is to identify the most efficient configuration for each type of nanogenerator based on their voltage output. Once the optimal material and mode are selected for PENG and contact-separation mode for TENG, these are integrated into a hybrid system.

A key contribution of this work lies in the design and simulation of a hybrid system circuit that converts the alternating current (AC) outputs of the nanogenerators into direct current (DC), suitable for charging a lithium-ion battery. Two full-wave bridge rectifier (FWBR) configurations, series and parallel FWBRs are implemented and compared in MATLAB Simulink to determine which offers more efficient energy conversion. This approach provides a practical insight not only into maximizing voltage output but also into achieving circuit-level optimization for real-world energy harvesting applications, offering a more complete and application-focused methodology than many prior works [1][7].

2.0 METHODOLOGY

The performance of a hybrid energy harvesting system that combines piezoelectric nanogenerators (PENGs) and triboelectric nanogenerators (TENGs) is systematically examined in this study. The methodology and process to optimize energy conversion efficiency and output performance involves circuit design and simulation modelling.

2.1 Modelling of Nanogenerators

COMSOL Multiphysics and MATLAB Simulink tools are used for modelling and simulation works in order to investigate and examines the hybrid nanogenerator system. The electrical performance of both PENGs and TENGs under various conditions is demonstrated by COMSOL Multiphysics software.

2.1.1 PENG Modelling

The simulations of piezoelectric nanogenerators evaluate the energy conversion efficiency of various materials, specifically lead zirconate titanate (PZT-5H) and polyvinylidene fluoride (PVDF). To evaluate these materials' capacity to generate voltage, mechanical forces of 735 Newton and 1470 Newton are applied. The applied mechanical forces of 735 N and 1470 N were selected to represent realistic load conditions, corresponding approximately to the weight of an average adult in Malaysia (75 kg) and the combined weight of two adults, respectively. These values simulate typical forces exerted during daily human activities such as walking or stepping, thereby providing practical relevance to the performance evaluation of the piezoelectric materials. The finite element analysis (FEA) in COMSOL Multiphysics software is used to evaluate the electrode potential, stress distribution and energy conversion efficiency. The best piezoelectric material to integrate into the single hybrid system is chosen based on the simulation findings, especially the voltage output generated from each material. The structure proposed piezoelectric nanogenerator considered under this study is as depicted in Figure 2.1.

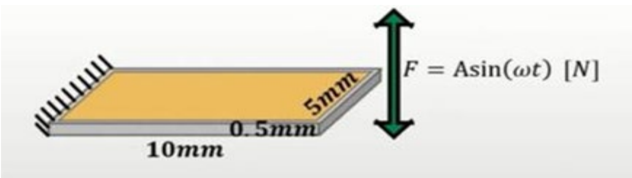

Figure 2.1 Structure of piezoelectric nanogenerator

The piezoelectric structure is designed with a length of 10 mm, a thickness of 0.5 mm, and a width of 5 mm to maximize mechanical deformation under an applied sinusoidal force. This particular geometry strikes a balance between flexibility and mechanical stability, ensuring efficient energy conversion while maintaining structural integrity. The 10 mm length provides sufficient surface area for energy harvesting, while the 0.5 mm thickness allows the material to exhibit adequate strain and flex in response to external forces. The 5 mm width is chosen to facilitate bending and enhance the strain induced in the piezoelectric material, which is essential for generating higher electrical output. Additionally, the selected dimensions are ideal for integrating the piezoelectric component with the triboelectric generator in the hybrid system, enhancing overall performance. The combination of these geometric features ensures that the nanogenerator can generate significant power while remaining mechanically stable, thus optimizing the energy-harvesting potential of the hybrid system.

In order to replicate realistic stresses like vibrations or external impacts, oscillating mechanical forces of 735 Newton and 1470 Newton are applied based on this force equation.

$$F = A\sin(\omega t) \tag{1}$$

where F is the applied force in sine function, A is the amplitude of the applied force, ω is the angular velocity that equal to $\omega = 2\pi f$ and f is the frequency applied which is 4 Hz to replicate and simulate low-frequency mechanical inputs. One side of the PENG structure is subjected to fixed boundary conditions to simulate its connection to a base structure, while the other side is subjected to the applied force.

The open circuit voltage, Voc of PENG simulation as shown in the equation.

$$Voc = k\frac{\sigma(z)}{\varepsilon} \quad (2)$$

where k is the thickness of piezoelectric medium, $\sigma(z)$ piezoelectric polarization charges and ε indicates multiplication between permittivity of free space, ε_0 which has constant value 8.854 x 10^{-12} F/m and relative permittivity, ε_r of the piezoelectric material applied, which are PZT-5H and PVDF materials.

2.1.2 TENG Modelling

The simulations of triboelectric nanogenerators investigate several operating or working modes such as single-electrode modes and contact-separation modes. Electric field distribution, open-circuit voltage production and charge transfer efficiency are determined by simulating the triboelectric effect and electrostatic induction of this triboelectric nanogenerators. An important indicator of performance, the open-circuit voltage (V_{OC}) and electrical field, E are computed based on this equation.

$$V_{OC} = \frac{\sigma x(t)}{\varepsilon_o \varepsilon_r} \quad (3)$$

where σ is the triboelectric charge surface density, *x(t)* distance between the dielectric from the primary electrode, ε_o permittivity of free space which has constant value 8.854 x 10^{-12} F/m and ε_r relative permittivity based on the triboelectric material applied, PTFE.

The electric field from the triboelectric nanogenerators mechanism can be calculated by using Equation (4).

$$E = -\frac{\sigma(z,t)}{\varepsilon_o \varepsilon_r} \quad (4)$$

where $\sigma(z, t)$ charge density at position z and time t, ε_0 permittivity of free space which has constant value 8.854x10^{-12} F/m and εr relative permittivity.

Table 2.1 Parameters used for single-electrode mode of triboelectric nanogenerator

Parameters	Values
Dielectric 1	ε_{r1} = 2, d_1 =100m
Thickness of electrodes, d_m	1 µm
Width of the structure, w	5 mm
Length of dielectrics, l	5 mm
Gap distance between electrodes, g	1 mm
Tribo-charge surface density, σ	8µ cm^{-2}
Maximum separation distance, x_{max}	0.020 m
Average velocity, v	1 m/s

Triboelectric interactions including materials like copper and polytetrafluoroethylene (PTFE). To maximize the energy production, the TENG's performance is evaluated under various gap distances and also different working modes as stated before, which are single-electrode modes (see Figure 2.2(a)) and contact-separation (see Figure 2.2(b)) modes.

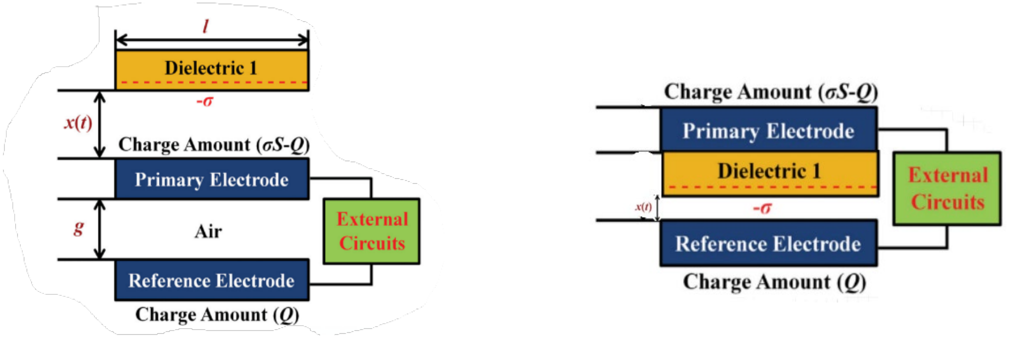

(a) Structure of single-electrode mode (b) Structure of contact-separation mode

Figure 2.2 Structure of triboelectric nanogenerator

The material for Dielectric 1 is PTFE material and material for both electrodes are copper electrodes. g is the air gap distance between primary and reference electrode and x(t) is distance between the dielectric from primary electrode which varied between 0.000 m to 0.020 m with increasing step of 0.001 m to simulate different mechanical inputs.

2.2 Designing of Single Hybrid Nanogenerator

To provide effective energy conversion and storage, piezoelectric nanogenerators (PENGs) and triboelectric nanogenerators (TENGs) must be electrically integrated. This process can be accomplished by converting alternating current (AC) output from both nanogenerators into direct current (DC) using full-wave bridge rectifiers (FWBRs), which makes the energy appropriate for real-world uses and storage. Rectification is required to create a consistent and stable DC output because PENGs and TENGs' naturally produce AC signals from their electromechanical energy conversion processes. Using MATLAB Simulink software, two different configurations of full-wave bridge rectifiers (FWBRs), which are series and parallel configurations are conducted, implemented and simulated in order to investigate their impacts on the hybrid system's voltage and current output. The effectiveness and suitability of the energy harvesting system in different electronic devices and storage solutions are greatly influenced by these configurations.

2.2.1 Series FWBRs Configuration

The voltage output generates by each of PENG and TENG components are summed, which resulting in higher and larger total voltage generation. This configuration guarantees that the sum of the individual voltages produced by the PENG and TENG components is the overall voltage output. The total output voltage and current of this configuration can be calculated using this equation:

$$V_{total} = V_{PENG} + V_{TENG} \quad (5)$$

$$I_{total} = I_{PENG} = I_{TENG} \quad (6)$$

Although this configuration is advantageous for applications requiring high voltage, it might not be the best choice in situations when high current is required because the current in the circuit remains constant. In low-power electronic applications that need greater voltage levels such as sensors and biomedical devices, the series FWBRs configuration is particularly beneficial. The structure of this design can be shown as in Figure 2.3 below.

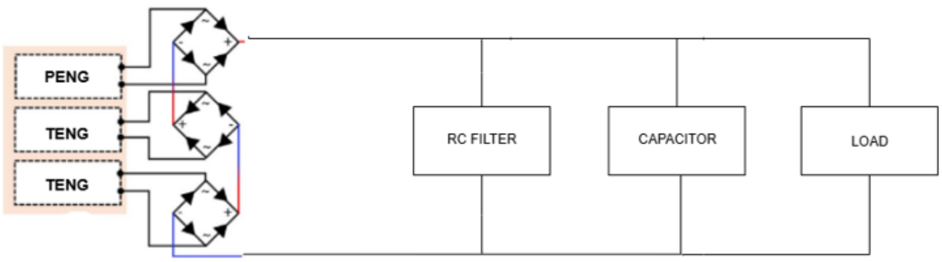

Figure 2.3 Block diagram of single hybrid system using series FWBR configuration

Based on Figure 2.3, the FWBR is also used for each nanogenerator in order to transform the alternating current (AC) from nanogenerator output into direct current (DC) before connecting them into series configurations.

2.2.2 Parallel FWBRs Configuration

In parallel configuration, both nanogenerators' output currents are combined, which keeps the system's voltage remains constant. The total output voltage and current of this configuration can be seen as stated by equation below:

$$V_{total} = V_{PENG} = V_{TENG} \tag{7}$$

$$I_{total} = I_{PENG} + I_{TENG} \tag{8}$$

Applications that require a larger current supply rather than high voltage supply are better suited for this design. The charging capability of the storage system is improved by connecting PENG and TENG components in parallel, which raises the overall current output. Due to the faster charging periods and improved battery performance from the higher current availability, the parallel design is well-suited for energy storage applications. Figure 2.4 depicts the block diagram of single hybrid system using parallel FWBR configuration.

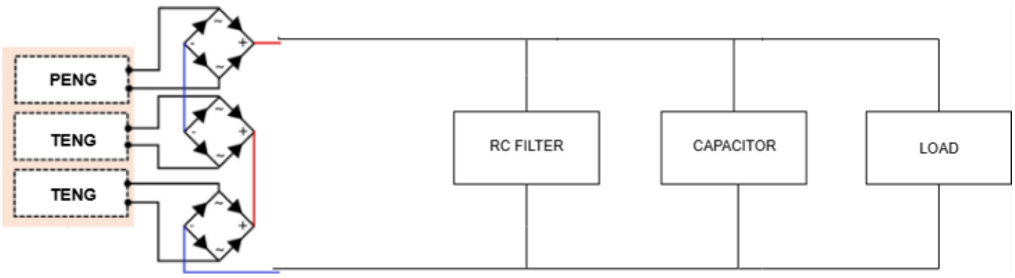

Figure 2.4 Block diagram of single hybrid system using parallel FWBR configuration

According to Figure 2.3 and 2.4, one PENG and two TENG are chosen in this single hybrid system in order to maximize the energy harvesting efficiency. Triboelectric nanogenerators typically provide a higher output than piezoelectric generators due to their enhanced charge generation through contact-separation mechanisms. By using two TENGs, the system benefits from a stronger and more consistent electrical output. The single PENG is included to complement the triboelectric generators, offering stability and helping to balance the overall system. This combination allows for a more efficient energy harvesting system that leverages the strengths of both technologies.

3.0 RESULTS AND DISCUSSIONS

The primary objective of these preliminary results is to evaluate the performance and energy harvesting efficiency of a hybrid nanogenerator system that integrates piezoelectric and triboelectric mechanisms. The evaluation focuses on the voltage output under various configurations and operating conditions, with simulations and measurements carried out as follows:

1. Measurement of voltage output from piezoelectric nanogenerators (PENGs) using different materials and applied force levels.
2. Measurement of voltage output from triboelectric nanogenerators (TENGs) under varying operational modes.
3. Measurement of output voltage from the proposed single hybrid nanogenerator circuit incorporating a series full-wave bridge rectifier (FWBR) configuration.

In this paper, focus has paid to the generated voltage only. This is crucial to identifying and analyzing the voltage output, as it serves as a primary indicator of the system's capability to generate sufficient electrical energy for practical applications. This parameter directly impacts the feasibility of integrating hybrid nanogenerators into low-power electronic devices such as sensors, wearables, and portable energy storage systems. Moreover, understanding voltage behavior under different material properties and configurations enables optimization for maximum energy conversion efficiency.

3.1 Piezoelectric Nanogenerator (PENG) Simulation

3.1.1 Material used: PZT-5H

Figure 3.1(a) and Figure 3.1(b) illustrate the PENG simulations conducted in COMSOL Multiphysics using PZT-5H material, under applied forces of 735 N and 1470 N, respectively. Under the lower force condition (735 N), the peak voltage attained is approximately 0.04 V, whereas doubling the force to 1470 N results in a peak voltage of 0.08 V. This outcome suggests a proportional relationship between the applied mechanical force and the output voltage generated by the PENG material.

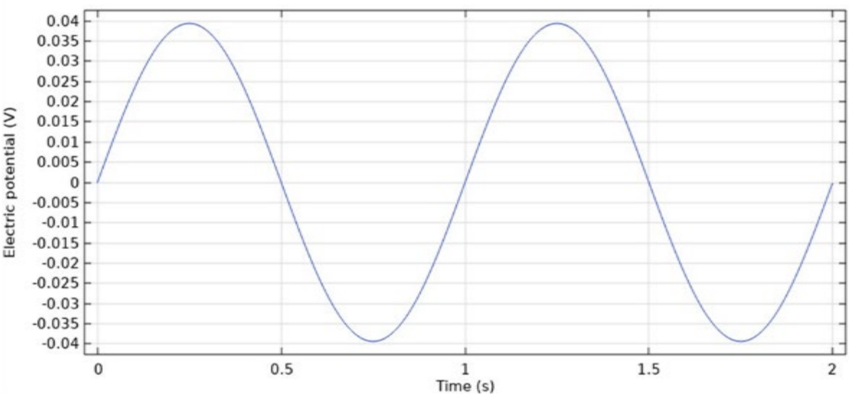

(a) Force applied = 735 Newton

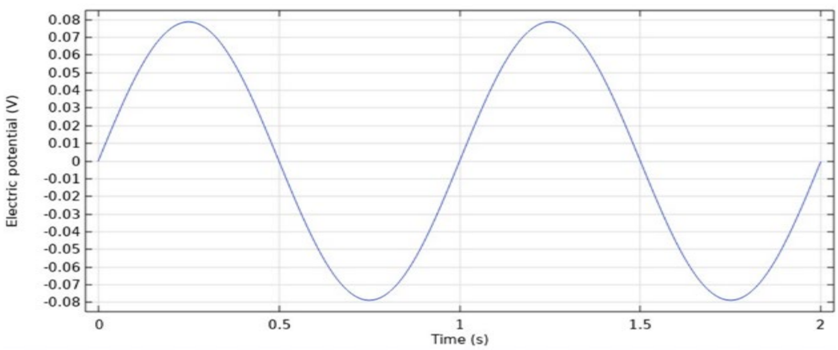

(b) Force applied = 1470 Newton

Figure 3.1 Voltage generated by PZT-5H material

3.1.2 Material used: PVDF

Figures 3.2(a) and Figure 3.2(b) present the results of PENG simulations conducted in COMSOL Multiphysics using PVDF material under applied mechanical stresses of 735 Newton and 1470 Newton, respectively, consistent with the previous simulations using PZT-5H. As shown in Figure 3.2(a), a peak voltage of 7.5 V is recorded under the lower force (735 Newton), while Figure 3.2(b) demonstrates a peak voltage of 14.5 V under the higher force (1470 Newton). These results further confirm that the PENG output is directly proportional to the applied mechanical stress. Additionally, a comparative analysis reveals that, under identical loading conditions, PVDF material generates a significantly higher voltage output than PZT-5H.

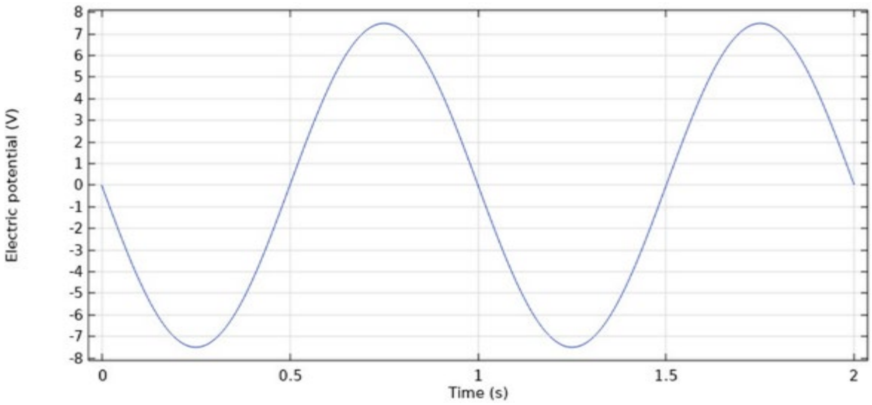

(a) Force applied = 735 Newton

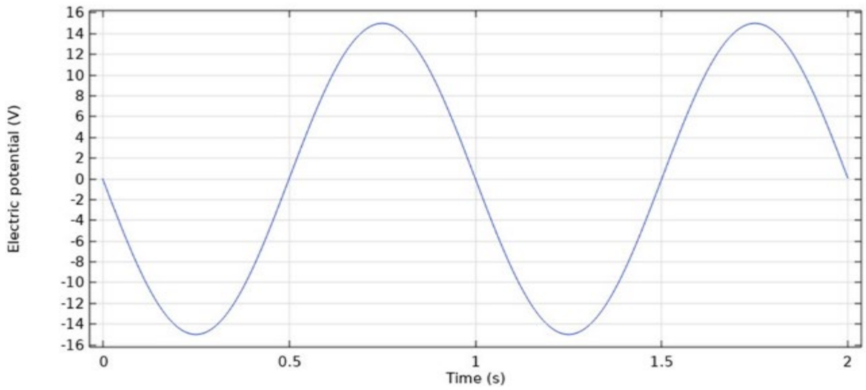

(b) Force applied = 1470 Newton

Figure 3.2 Voltage generated by PVDF material

Simulation results show that PVDF material produced significantly higher voltages (up to 14.5 V at 1470 N) compared to PZT-5H (0.08 V at the same force). This is in line with findings by He et al. (2024) [7] and Wang et al. (2023) [8], who noted that flexible polymers like PVDF, despite lower piezoelectric coefficients, often exhibit higher voltages due to their larger deformation under stress and better mechanical matching in hybrid systems.

3.2 Triboelectric Nanogenerator (TENG) Simulation

Figures 3.3(a) to Figure 3.3(c) present the results of triboelectric effect simulations conducted in COMSOL Multiphysics using the single-electrode mode configuration. Figures specifically illustrate the electric potential generated as the dielectric material moves progressively farther from both the primary and reference electrodes. The separation distances between the dielectric and the primary electrode are 0.000 m, 0.005 m, and 0.010 m for Figure 3.3(a), Figure 3.3(b) and Figure 3.3(c), respectively.

The specific separation distances selected for simulation 0.000 m, 0.005 m, and 0.010 m were chosen to represent a realistic range of mechanical displacements found in typical triboelectric applications such as human walking, hand tapping, or environmental vibrations. Studies by Guo et al. (2020) [2] and Bai et al. (2020) [3] have shown that gap distances between 1 mm and 10 mm are common in wearable and vibration-based TENG designs due to their mechanical feasibility and effective voltage output. Moreover, previous benchmarking from Wang et al. (2019) [1] and Li et al. (2020) [10] suggests that this range also offers an optimal balance between performance enhancement and electrical stability, avoiding the onset of air breakdown or excessive charge leakage at higher distances.

The simulation results indicate that as the dielectric material moves farther from the primary electrode, the areas represented by red and blue regions expand, signifying an increase in the generated electric potential. The red region corresponds to the maximum electric potential ($V_{positive}$), while the blue region represents the minimum electric potential ($V_{negative}$).

The combined effect of these potentials is illustrated by the waveform in Figure 3.4, which shows that the maximum open-circuit voltage (V_{oc}) achievable in the single-electrode triboelectric configuration is approximately 300 V. These findings demonstrate that increasing the separation distance between the dielectric and the primary electrode enhances the open-circuit voltage output.

(a) when distance dielectric from both electrodes is 0.000 meter

(b) when distance dielectric from both electrodes is 0.005 meter

(c) when distance dielectric from both electrodes is 0.010 meter

Figure 3.3 Contour region of electric potential results in COMSOL Multiphysics software, for different distance between dielectric and electrodes

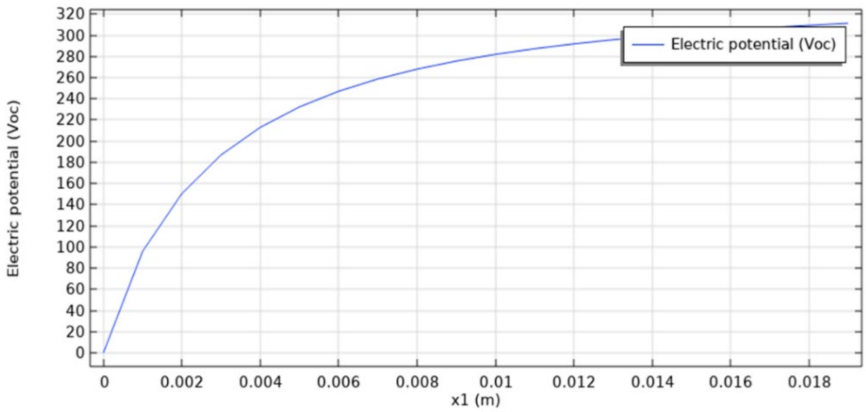

Figure 3.4 Open-circuit voltage waveform generated for single-electrode mode

Figures 3.5(a) to Figure 3.5(c) present the results of triboelectric effect simulations conducted in COMSOL Multiphysics using the contact-separation mode configuration. Figures 3.5(a), 3.5(b) and 3.5(c) specifically illustrate the electric potential distribution as the dielectric material, attached to the primary electrode, moves progressively away from the reference electrode. The separation distances between the dielectric and the reference electrode are 0.000 m, 0.005 m, and 0.010 m for Figures 3.5(a) to 3.5(c), respectively.

The simulation results show that as the dielectric material attached to the primary electrode moves farther from the reference electrode, the red regions (representing areas of high electric potential) expand more significantly than the blue regions. This indicates an increase in the generated electric potential, particularly the maximum electric potential ($V_{positive}$). The combined maximum and minimum electric potentials are represented by the waveform in Figure 3.6. From this, it can be observed that the maximum open-circuit voltage (V_{oc}) achieved in the contact-separation triboelectric mode is approximately 3892.2 V. These results clearly demonstrate that increasing the separation distance between the dielectric material and the reference electrode leads to a higher open-circuit voltage.

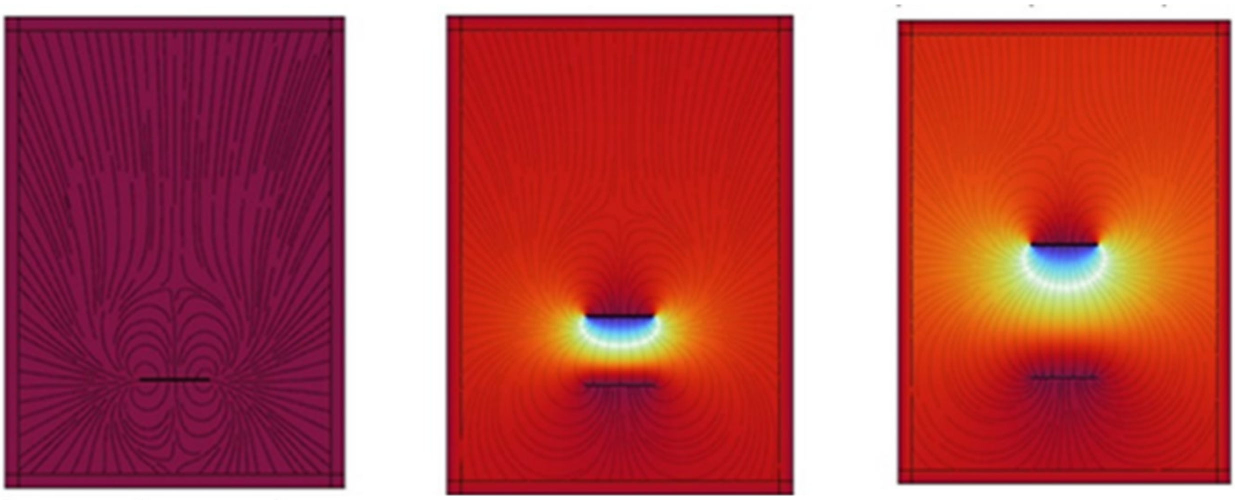

(a) when distance dielectric attached with primary electrode moves away from reference electrode is 0.000 meter

(b) when distance dielectric attached with primary electrode moves away from reference electrode is 0.005 meter

(c) when distance dielectric attached with primary electrode moves away from reference electrode is 0.010 meter

Figure 3.5 Contour region of electric potential results in COMSOL Multiphysics software, for different distance dielectric attached with primary electrode moves away from reference electrode

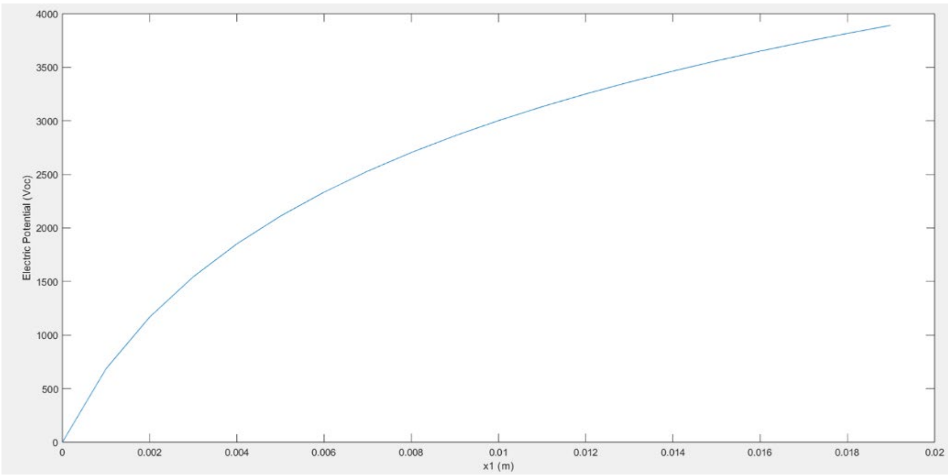

Figure 3.6 Open-circuit voltage waveform generated for contact-separation mode

Based on Figure 3.4, in the single-electrode mode, the open-circuit voltage waveform reached a maximum value of approximately 300 V at a 0.010 m gap. Although this is lower than the voltage observed in the contact-separation mode, it is consistent with the behavior described in triboelectric theory and supported by comparative studies. In this mode, one electrode remains grounded, and the charge transfer depends more heavily on the surrounding environment, which typically limits the achievable voltage compared to symmetric modes like contact-separation. According to Yang et al. (2013) [5] and Sriphan & Vittayakorn (2022) [6], the single-electrode mode, while mechanically simpler, usually delivers lower voltage output due to partial grounding and reduced electric field concentration across the dielectric interface. This mode is generally used in compact or flexible designs where simplicity and integration outweigh peak performance. Nonetheless, the observed increase in voltage as separation increases still validates the theoretical model and supports prior conclusions about distance-dependence in triboelectric interactions [5] [6].

Next, for Figure 3.6, the simulation results align closely with theoretical predictions and experimental benchmarks reported in existing literature. In the contact-separation mode, the open-circuit voltage peaked at approximately 3892.2 V when the separation distance reached 0.010 m, a marked increase from the lower voltages observed at 0.000 m and 0.005 m. This voltage amplification with increasing distance is theoretically explained by the triboelectric model, where the open-circuit voltage is proportional to the separation distance, as described by equation (3) . This relationship is well-supported in prior studies, including Wang et al. (2019) [1] and Li et al. (2020) [10], which confirmed that larger displacements in contact-separation TENGs lead to significantly higher potential differences due to more efficient electrostatic induction. For instance, Li et al. observed voltage increases of over 1000% as the separation distance was increased from 1 mm to 10 mm in their experimental setup [1] [10]. Furthermore, Guo et al. (2020) [12] emphasized that an optimal separation range of 5–15 mm offers high voltage output while maintaining device stability and preventing dielectric breakdown. These findings affirm the accuracy of the simulation results presented in this study and underline the importance of optimizing mechanical displacement in TENG design for enhanced performance.

3.3 Single Hybrid Nanogenerator Simulation

Figure 3.7 presents the output waveforms generated in MATLAB Simulink for the proposed single hybrid nanogenerator circuit, which employs a series full-wave bridge rectifier (FWBR) configuration. The top three waveforms represent the AC voltage outputs generated individually by one piezoelectric nanogenerator (PENG) and two triboelectric nanogenerators (TENGs). The bottom waveform illustrates the combined output of the hybrid system after rectification through the series FWBR configuration. Specifically, the first waveform corresponds to the AC output from the PENG, while the second and third waveforms represent the AC outputs from the two TENGs. Following the integration and rectification of the nanogenerators (1 PENG and 2 TENGs), the resulting output (as depicted in the fourth waveform) demonstrates a DC voltage waveform. This rectified output is suitable for direct use in a lithium-ion battery charging system.

(a)

(b)

(c)

(d)

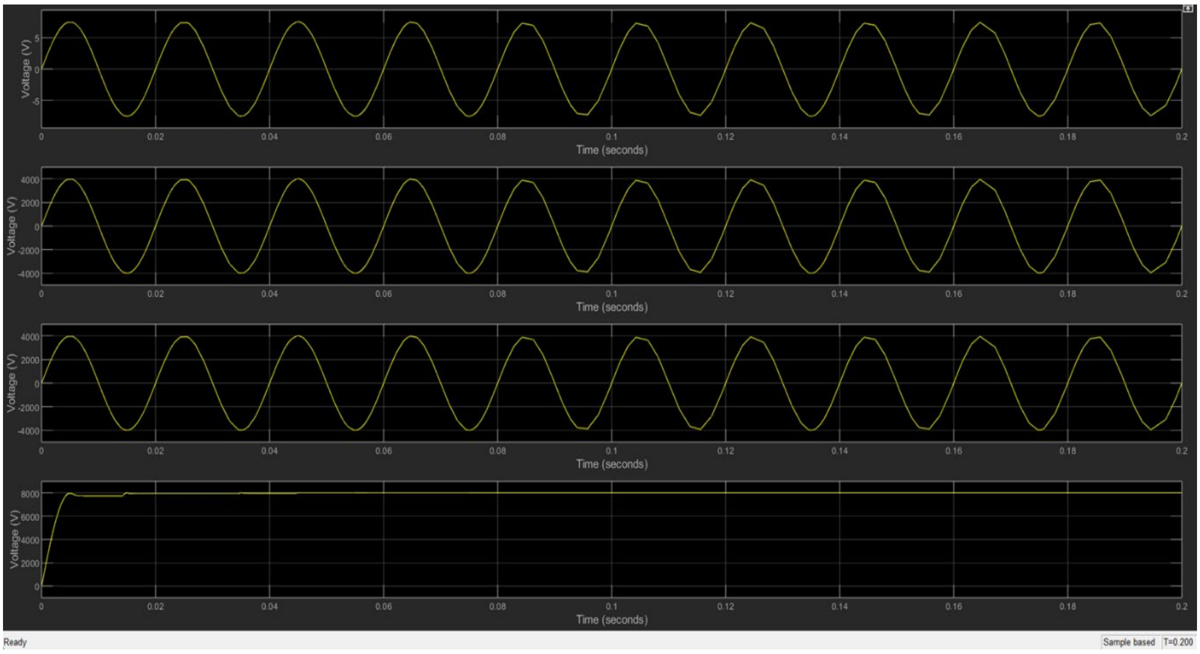

Figure 3.7 Voltage output waveform of single hybrid system using series FWBRs configuration in MATLAB Simulink software, (a) Generated voltage for PENG (b) Generated voltage for the first TENG (c) Generated voltage for second TENG (d) The rectified output voltage of the hybrid nanogenerator systems

This results in an overall voltage that is the arithmetic sum of the individual voltages a depicted in Figure 3.7(d). Such design is beneficial for applications requiring high voltage but moderate current, such as sensor nodes or biomedical implants. This approach has been validated in previous studies. Yang et al. (2013) [5] and He & Briscoe (2024) [7] demonstrated that hybrid nanogenerators show improved power density and energy conversion efficiency when the outputs are conditioned through proper rectification circuits like FWBRs. Similarly, Sriphan & Vittayakorn (2022) [6] emphasized the importance of electrical integration in hybrid systems, noting that series rectification maximizes voltage output, which is particularly advantageous in scenarios where space is limited but voltage requirements are high.

Moreover, the decision to use two TENGs and one PENG in this hybrid configuration follows a strategy recommended in recent works, such as by Sari et al. (2023) [13], where system stability and high voltage output were achieved through redundancy and complementary energy generation. The TENGs, known for their high voltage but intermittent output, complement the PENG's more stable but lower voltage output, producing a balanced and robust energy harvesting system.

In conclusion, the simulation outcomes not only confirm the operational synergy of the hybrid nanogenerator but also align well with theoretical models and prior research. The combination of PENG and TENG, rectified through a FWBR circuit, demonstrates significant potential in delivering a stable and efficient DC output for use in low-power electronic systems.

4.0 CONCLUSION

In conclusion, the research findings demonstrate that hybrid nanogenerator systems—by combining piezoelectric and triboelectric nanogenerators, named as hybrid nanogenerators—offer significant potential for enhancing energy harvesting efficiency. By integrating both technologies, the hybrid system effectively optimizes voltage and current generation, leveraging the strengths of each mechanism. Simulation results reveal that PVDF-based PENGs produce a higher voltage output compared to those using PZT-5H material. Additionally, TENGs exhibit superior performance in the contact-separation mode as opposed to the single-electrode configuration. Furthermore, the use of series full-wave bridge rectifiers (FWBRs) enhances the hybrid system's performance by increasing the overall voltage output. These results collectively underscore the feasibility and practicality of employing hybrid nanogenerators for powering portable and wearable electronic devices, thereby contributing to the advancement of sustainable and environmentally friendly energy solutions.

For future work, the multilayer arrangement or stacking of PENG and TENG components could be investigated to further enhance energy output. Such configurations may increase the effective surface area for energy conversion, thereby enabling greater efficiency and broader applicability in real-world scenarios.

ACKNOWLEDGEMENTS

The authors would like to express their appreciation for the support of the sponsors with project no. R.J130000.7323.1R008, Agency Grant (sponsored by JKR Create Melaka), the Q.J130000.3023.04M68, Matching Grant (sponsored by UTM) and R.J130000.7809.5F736, Fundamental Research Grant Scheme (FRGS), sponsored by the Ministry of Higher Education, Malaysia.

REFERENCES

[1] Wang, Z. L., & Wang, A. C. (2019). Triboelectric nanogenerators as new energy technology for self-powered systems and as active mechanical and chemical sensors. Nature Reviews Materials, 5(7), 351-370. https://doi.org/10.1038/s41578-019-0155-3

[2] Guo, H., Yeh, M.-H., Lai, Y.-C., Bai, P., Lin, Z.-H., & Wang, Z. L. (2020). Triboelectric Nanogenerator for Sustainable Energy and Environment. *Nature Communications*. National Center for Biotechnology Information. https://doi.org/10.1038/ncomms8376

[3] Bai, P., Zhu, G., Lin, Z.-H., Jing, Q., Chen, J., Zhang, G., Ma, J., & Wang, Z. L. (2020). Integrated Multilayered Triboelectric Nanogenerator for Harvesting Wind Energy. *ACS Nano*. National Center for Biotechnology Information. https://doi.org/10.1021/nn503139v

[4] Dhakar, L., Tay, F. E. H., Lee, C., & Wang, Z. L. (2016). Piezoelectric energy harvesting from human walking and running. Energy & Environmental Science, 9(3), 922-931. https://doi.org/10.1039/C5EE03178A

[5] Yang, Y., et al. (2013). A hybrid energy cell for self-powered water splitting. Energy & Environmental Science, 6(8), 2429-2434. https://doi.org/10.1039/C3EE40899A

[6] Sriphan, S., & Vittayakorn, N. (2022). Hybrid piezoelectric-triboelectric nanogenerators for flexible electronics: Recent advances and perspectives. *Journal of Science: Advanced Materials and Devices, 7*(3), 100–115. https://doi.org/10.1016/j.jsamd.2022.100123

[7] He, Q., & Briscoe, J. (2024). Piezoelectric energy harvester technologies: Synthesis, mechanisms, and multifunctional applications. ACS Applied Materials & Interfaces, 16(23), 29491–29520. https://doi.org/10.1021/acsami.3c17037

[8] Wang, Z., Liu, Y., & Yang, P. (2023). Design and optimization of piezoelectric nanogenerators for high-performance energy harvesting. *Nano Energy*, 104, 107920. https://doi.org/10.1016/j.nanoen.2023.107920

[9] Tribonet. (2023). Triboelectric Nano Generators - TENG - About Tribology. Retrieved from Tribonet.

[10] Li, X., Zhang, H., Wang, Z. L., & Yu, A. (2020). Triboelectric nanogenerator: Structure, mechanism, and applications. *ACS Nano, 14*(1), 1–12. https://doi.org/10.1021/acsnano.0c09823

[11] Sari, E. A., Rachmat, M., & Widiastuti, F. (2023). Recent Developments in Piezoelectric Nanogenerators: A Systematic Review. *Nanomaterials*, 3(2), 7. MDPI. https://doi.org/10.3390/nanomaterials3020007

[12] Guo, H., Yeh, M.-H., Lai, Y.-C., Bai, P., Lin, Z.-H., & Wang, Z. L. (2020). Triboelectric Nanogenerator for Sustainable Energy and Environment. *Nature Communications*. National Center for Biotechnology Information. https://doi.org/10.1038/ncomms8376

[13] Sari, E. A., Rachmat, M., & Widiastuti, F. (2023). Recent Developments in Piezoelectric Nanogenerators: A Systematic Review. *Nanomaterials*, 3(2), 7. MDPI. https://doi.org/10.3390/nanomaterials3020007